https://doi.org/10.22226/2410-3535-2022-4-292-297

Atypical behavior of materials during current-assisted tension

V. V. Stolyarov

vlstol@mail.ru

Mechanical Engineering Research Institute of the RAS, Moscow, 101990, Russia

The passage of electric current in conductive materials is accompanied by a variety of physical phenomena, one of which is the so-called electroplastic effect, which manifests itself in a decrease in flow stresses and an increase in plasticity. Despite the early discovery of the electroplastic effect, the proposed mechanisms could not fully explain the observed experimental facts. Moreover, as shown in this study, some modes/regimes of electric current can lead to atypical strengthening phenomena even in pure metals and to atypical upward stress jumps in alloys with phase transformations. The paper considers examples of strengthening under a pulsed current with a density greater than the critical one and a duty cycle of more than 10^3 in pure metals, shape memory alloys, ferrite-pearlitic and stainless steels. It is assumed the selected current regimes provide the minimum thermal effect and maximum stress relaxation. The literature data and the results obtained, suggests that among the possible causes of strengthening there may be structural changes (recrystallization and refinement of grains, transformation of lamellar phases into spherical ones), martensitic transformation. It is concluded the atypical current effect is due to the material nature and high duty cycle of the electric current.

Keywords: metals, alloys, tension, pulse current, strengthening, electroplastic effect.

1. Introduction

It is known that the passage of electric current in conductive materials is accompanied by thermal (Joule effect), optical, electromagnetic (skin and pinch effects), and mechanical (vibration) phenomena [1–3]. Particularly interesting and practically important for the development of new processing technologies is the mechanical behavior of metallic materials, for example, during tension accompanied by a pulsed current. It has been called the electroplastic effect (EPE) and has been studied in detail in many pure metals (Zn, Cd, Pb, Sn, Ti, Cu) and thermally stable alloys based on titanium (Ti64), magnesium (AZ31), aluminum (AA6000 and AA7000), copper (brass), and iron (austenitic steels) [1–8]. It was found that single current pulses (duty cycle $q \gg 10$) led to the appearance of downward stress jumps on the tensile curve. It was argued that EPE was a combination of the above phenomena that acted simultaneously, but might have different relative contributions [1–3]. A typical EPE manifestation upon the introduction of a multipulse current ($q \leq 10$) also consists in a decrease in flow stresses and an increase in plasticity for different deformation schemes [4–8].

The practical significance of EPE is due to the possibility of eliminating the intermediate stages of annealing and deformation in metalworking processes. The scientific significance of EPE is associated with the need to understand the physical mechanisms of plastic deformation when interacting with an electric current. Previously, the influence of the current mode [9], current regimes [10], the accompanying thermal effect [11], and the material itself [12] on the mechanical properties of the metal was shown. In most of these studies, the materials exhibited softening and increased ductility without significant heating. Several mechanisms have been proposed to explain the observed effects. These include thermal heating [11], the magnetoplastic effect [13], and the interaction of free electrons with mobile or pinned dislocations [3]. The above mechanisms satisfactorily explain the softening effect of the current in pure metals or single-phase alloys without structure-phase transformations. In all cases, tensile deformation in the presence of current was accompanied by either downward stress jumps or a decrease in flow stresses at a current density above the critical value [3]. This practically important property of the current has been widely used in the practice of metalworking, and its effectiveness has also been shown to suppress serrated deformation (the Portevin-Le Chatelier effect) in AMg6 aluminum alloys [14,15].

In more complex materials, such as multiphase alloys, steels with martensitic transformation, aging alloys and intermetallics, the interpretation of EPE may not be so clear and unambiguous. It turned out that in a number of cases anomalous strengthening effects could be observed that was caused either by special current regimes or by the nature of the materials under study. For the first time, strengthening under tension accompanied by a pulsed current was observed in $Ti_{49.3}Ni_{50.7}$ shape memory alloys [16]. It was noted that upward stress jumps (with an amplitude of up to 150 MPa) were recorded on the tensile curves in the plateau region and beyond when single high-density current pulses ($j = 550$ A/mm^2) were introduced. In the case of application of direct or multipulse current of low density, there were no jumps, but strengthening was also observed, albeit to a lesser extent. In a recent work [17], strengthening was also observed in a coarse-grained Ti-7 at.% Al alloy (hcp) with the introduction of a multipulse current with a density of

5 A/mm^2. The authors interpret the effect of strengthening by the special nature of the alloy, by changing the deformation mechanism from slip to twinning and provide structural evidence for dislocation climbing. Strengthening caused by electropulse processing (without deformation) was observed in medium-carbon and ferritic-pearlitic steels [18,19]. Of a particular interest are thermally unstable alloys, in which structural-phase transformations are possible during heating or deformation [20,21].

In this regard, the purpose of the article is to demonstrate an atypical (anomalous) tensile deformation behavior accompanied by a high duty cycle pulsed current in materials of various nature.

2. Materials and experimental methods

The materials studied were pure metals (titanium and aluminum) and shape memory alloys based on TiNi and steel. Titanium VT1-0 and VT1-00 with an impurity content of 0.3% and 0.1%, respectively, were used in the form of a wire with the diameter of 1 mm and a grain size of 20 μm. Aluminum was a single-crystal plate obtained under weightless conditions. Quenched coarse-grained (d = 20 μm) $Ti_{49.3}Ni_{50.7}$ and $Ti_{50}Ni_{50}$ alloys had the shape of a sheet. Low-carbon ferrite-pearlitic steel St3 was in the form of a drawn wire with the diameter of 1.5 mm, and austenitic chromium-nickel steel Cr6Ni4 in the form of strips. All materials, except steel wire, had an annealed coarse-grained state. The working part of the tensile specimens had a cross section of 2 mm^2. Since the actual length of the samples for different materials differed, the same gauge length l_0 = 25 mm was taken when calculating the relative elongation.

The tensile tests were carried out at room temperature and at a speed of 1 mm/min on a horizontal machine IR 5081-20. Tension in most cases was performed after stabilization of the temperature on the sample. In one case, tension was started simultaneously with the introduction of current. The current supply circuit is shown in Fig. 1a.

We used single current pulses of high density ($j > j_{cr}$) and duty cycle $q = T/\tau = 1/\nu\tau$, where T, τ and ν period, duration and frequency of pulses. An explanation for high duty cycle current, as well as schematic and real oscillograms, are shown in Fig. 1b,c. Current density, j, pulse duration, τ, and the duty cycle, q, were varied in accordance with the electrical resistivity and thermal conductivity of the materials under study so that the heating of the sample during the tensile time would be minimal, and stress jumps would be observed visually. The sample temperature was controlled by a thermocouple and an infrared camera. The discrepancy between the measured temperatures did not exceed ±5°C. Appropriate regimes, methods of current injection and actual sample temperatures are indicated in Table 1.

3. Results

Figure 2 shows stress-strain curves of commercial pure titanium VT1-0 and VT1-00 (Fig. 2a,b) and single-crystal aluminum (Fig. 2c) without current (curves 1) and with current in the form of single pulses (curves 2). In the case of the VT1-0 alloy, the current was introduced simultaneously with tension (Fig. 2a).

Curves 2 show downward stress jumps corresponding to single current pulses. When current is introduced simultaneously with the beginning of tension, stress jumps appear both in the elastic and plastic zones (Fig. 2a). The amplitude of the jumps depends on the material and current density, is about 10% of the effective flow stress and equal to 40 MPa for titanium and 5 MPa for aluminum. It can be seen that the introduction of current pulses in titanium and aluminum led to strengthening: the tensile strength increases

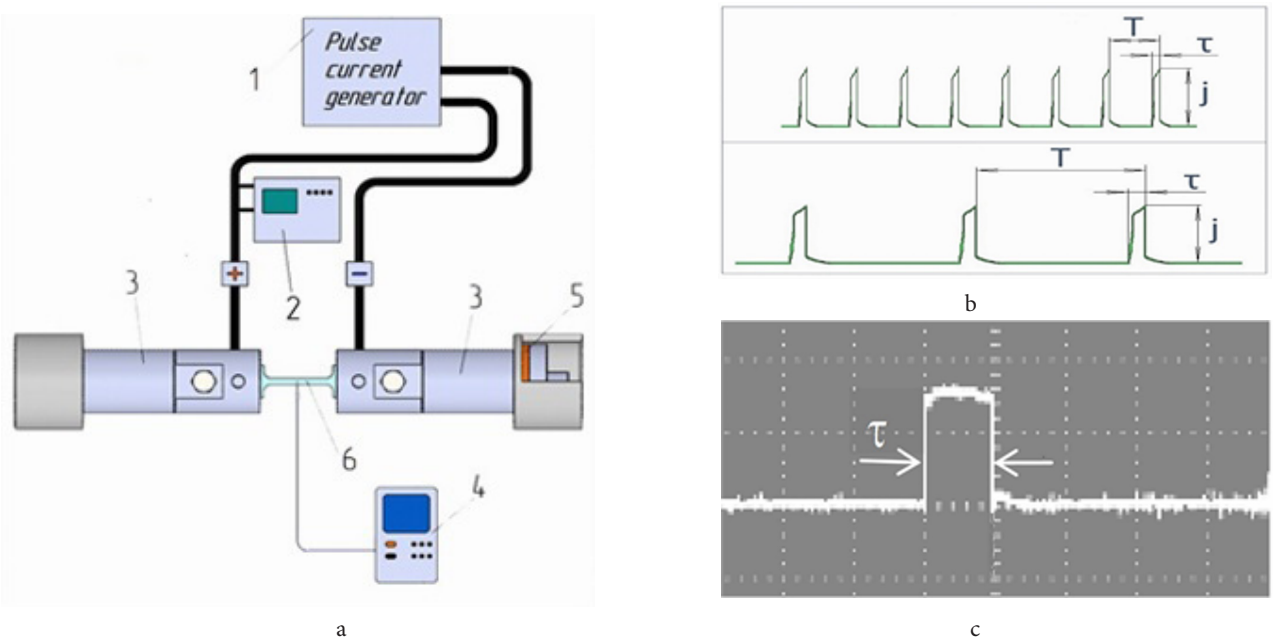

Fig. 1. (Color online) A scheme of the current supply (a) and oscillograms (b, c) at tension: 1 — pulse current generator; 2 — oscillograph; 3 — clamps of testing machine; 4 — thermocouple; 5 — insulation; 6 — specimen; b — schematic diagrams (up — low duty cycle, down — high duty cycle); actual oscillograms for high duty cycle (c).

Table 1. Regimes of pulse current for different materials.

Current regimes	VT1-0	VT1-00	Al single	$Ti_{49.3}Ni_{50.7}$	$Ti_{50}Ni_{50}$	St3	Cr6Ni4/sample
Density, A/mm^2	250	250	450	500	500	280	820 (#2) 2630 (#3)
Pulse duration, ms	1000	1000	1000	1000	1000	1000	250 (#2) 1000 (#3)
Duty cycle	20×10^3	20×10^3	2×10^3	13×10^3	5×10^3	2×10^3	10×10^3
Current introduction	with tension	before tension	before tension	before tension	before tension	before tension	before tension
Temperature,°C	26	25	23	50	38	51	54

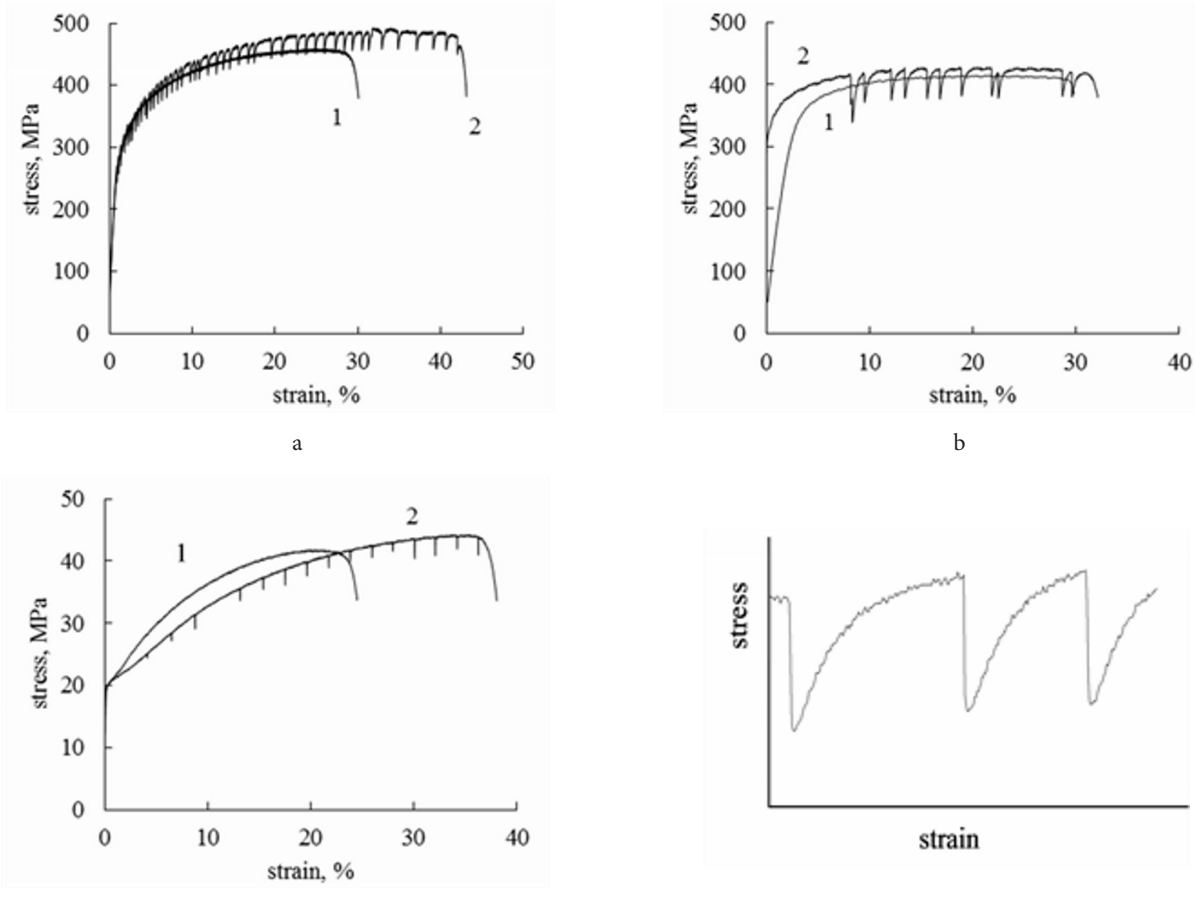

Fig. 2. Tensile stress-strain curves (a, b, c) and typical shape of stress jumps in titanium (d): VT1-0 (a); VT1-00 (b); Al single crystal. 1 — without current; 2 — single current pulses.

by 20 and 4 MPa, respectively, as compared to that of samples tested without current. The shape of the stress jump is asymmetric, the descending curve has a greater slope than the ascending one (Fig. 2 d). The relative elongation in the VT1-0 alloy and single-crystal aluminum also increased by 15 (30) %, while in VT1-00 it did not change. A characteristic feature of current-carrying curves is high uniform elongation without necking. Note that the temperatures of the samples during tension with and without current practically did not differ from room temperature (Table 1).

Let us consider now the deformation behavior of TiNi shape memory alloys. The strengthening effect was most pronounced in the austenitic post-stoichiometric alloy $Ti_{49.3}Ni_{50.7}$ (Fig. 3 a).

It can be seen that curve 2 (with single current pulses) at the beginning of deformation is 200 MPa higher than curve 1 (without current). As the strain increases, the strengthening effect (amplitude of stress jumps) decreases and disappears. The shape of stress jumps is also asymmetric; however, their direction is different from that in pure metals where it is downward. Note that the temperature of the sample at the time of the passage of the pulse increased to 50°C. However, in the equiatomic martensitic alloy of similar composition $Ti_{50}Ni_{50}$, there was no effect of strengthening, the stress jumps had amplitude of no more than 20 MPa and were directed downwards (Fig. 3 b). It is interesting that in this case, in different parts of the loading curve with current, there are multidirectional stress jumps: on the plateau stage it is downward, while on the stage of strain strengthening it is upward. Instead of strengthening in the alloy, the introduction of a pulsed current leads to a decrease in elongation to failure

and softening, this is especially noticeable with an increase of the strain.

The deformation curves of two types of steels, ferrite-pearlitic steel St3 and austenitic chromium-nickel steel Cr6Ni4, are shown in Fig. 4 a, b.

Here, as in the previous materials, the introduction of a pulsed current during tension led to different strengthening intensities and to a significant decrease in ductility. The introduction of current after the yield point caused a sharp decrease in the flow stresses in a short region of deformation curve, and then resulted in a long stage of strengthening by 30 – 40 MPa (Fig. 4 a).

Stronger strengthening up to 100 –150 MPa was observed in austenitic chromium-nickel steel (Fig. 4 b, curve 2) when a low current density was used, at which the amplitude of the jumps was hardly visible. A smaller strengthening effect (60 – 70 MPa) was observed at a higher current density (Fig. 4 b, curve 3).

4. Discussion

As studies have shown, the deformation behavior of materials under tension accompanied by a pulsed current can radically differ from the traditionally observed, well-known electroplastic effect. It consists in the general strengthening (instead of the usual softening), the value of which varies from several to hundreds of megapascals, as well as in the direction of stress jumps upwards (instead of the usual downwards) on the tensile curves. The observation of these features depends both on the regimes of the pulsed current and on the physical nature of the material. In this work, for all the studied materials, a pulsed current of a large duty cycle was used, the value of which was 10^3 –10^4. It seems that this condition plays a key role in experiments, since it ensures minimal heating, an equilibrium structure state, stress relaxation and a uniform distribution of the heat flux in the sample after the passage of each pulse. Note that with rare exceptions [3] in most similar studies, the authors used direct current, single current pulses, or pulsed current with a two to three orders of magnitude lower values of duty cycle.

As for the effect of the material, the interpretation of the observed strengthening in pure metals (Fig. 2) without analyzing structure studies is the most difficult, since phase transformations in them at temperatures close to room temperature do not occur. It can be assumed that the observed strengthening in aluminum and titanium is associated with low-cycle fatigue caused by low-frequency pulsed current (Fig. 2 a, b, c). Thermomechanical cycling leads to the accumulation of internal stresses and, accordingly, to strengthening. Noteworthy is the explanation associated with the change in the mechanism of slip deformation to dislocation climbing, which promotes twinning and strengthening. Such

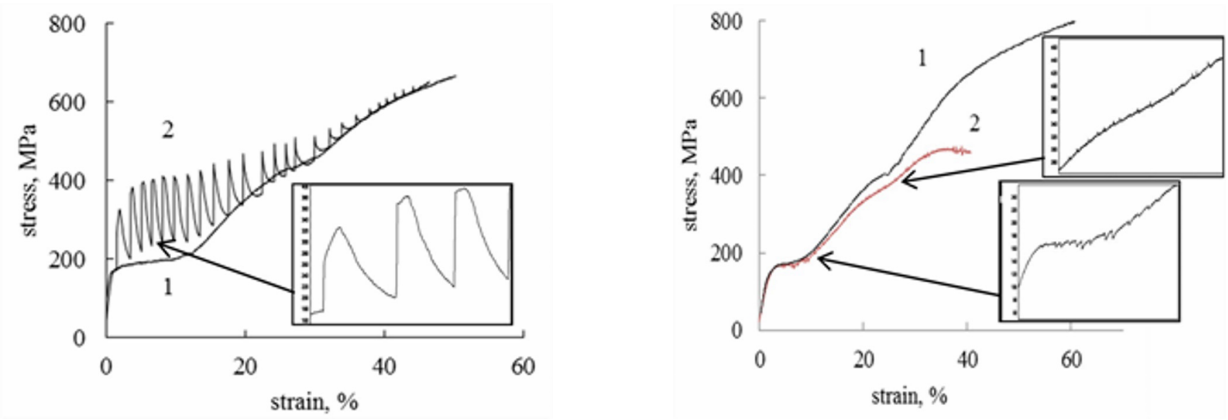

Fig. 3. Tensile stress-strain curves: $Ti_{49.3}Ni_{50.7}$ (a); $Ti_{50}Ni_{50}$ (b). 1 — without current; 2 — with current. Inserts: tensile diagram fragments.

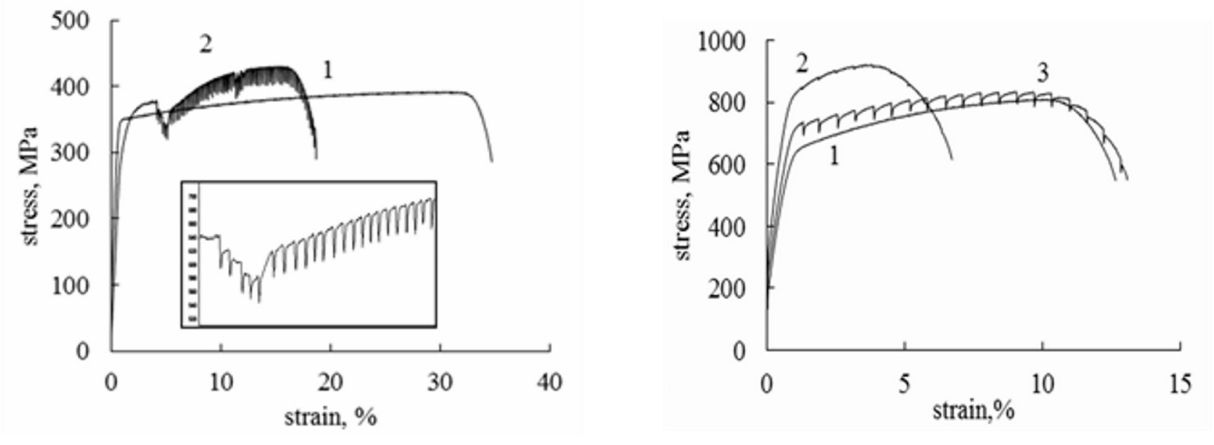

Fig. 4. Tensile stress-strain curves for steels St3 (a) and Cr6Ni4 (b): 1 — without current; 2, 3 — with current. In the insert to Fig. 4 a — a fragment of curve 2 on an enlarged scale.

a mechanism for a single-phase Ti-7Al at.% alloy having an hcp lattice, like titanium, was proposed by the authors of [17].

The different content of impurities in titanium VT1-0 and VT1-00 affected not only the strength characteristics, but also the effect of pulsed current. Unexpectedly, it turned out that in VT1-0 titanium with a high content of impurities, the increase in relative elongation due to current was greater than in VT1-00 titanium (Fig. 2 a, b). Probably, a higher content of impurities increases the electrical resistivity and the corresponding contribution of the thermal effect to plasticity.

In a single crystal of aluminum, the pulsed current caused a clearly visible decrease in work strengthening, an increase in uniform deformation, and a simultaneous increase in strength and ductility (Fig. 2 c). Such a response of the material is consistent with the possible healing of defects in it [18].

An analysis of the asymmetric shape of the stress jump allows one to assume that the intensity of stress reduction is one or two orders of magnitude higher than the intensity of its recovery (Fig. 2 d). This fact is due to the different speeds of the dislocation mechanisms acting at the moment of introduction (electronic "wind") and the end of the current pulse (local strain strengthening).

Next, alloys and steels will be considered in which phase transformations can occur as a result of deformation, heating, or both factors together. One example of such a material is shape memory alloys of the Ti-Ni system, which experience elastic reversible martensitic transformations [16]. Depending on the chemical composition of the alloy, the temperatures of the onset of the direct Ms and reverse As transformations of such alloys can vary over a wide range. In an alloy austenitic at room temperature, $Ti_{49.3}Ni_{50.7}$ ($M_s \geq RT$), plastic deformation causes the transformation of austenite A into martensite M, which appears as a plateau on the deformation curve (Fig. 3 a). The introduction of single current pulses in the plateau zone causes upward stress jumps due to an increase in the temperature of sample up to 50°C, reverse transformation M→A and higher flow stress in austenite [16]. With increasing strain, the stability of martensite increases, which leads to a decrease in the amplitude of stress jumps. As in the previous cases, the shape of the stress jump is asymmetric and is determined by the heating/cooling rate of the sample.

In the $Ti_{50}Ni_{50}$ martensitic alloy ($50°C \leq M_s \leq 100°C$) plastic deformation at room temperature in the plateau zone and weak heating with the introduction of current pulses cannot cause M→A transformation. As a result, the downward stress drops at the plateau stage are a consequence of the traditional EPE influence (Fig. 3 b). An increase in the strain reduces the stability of martensite, contributes to a weak M→A transformation under the action of current pulses and the appearance of upward jumps (Fig. 3 b). Due to the lamellar structure of martensite, downward stress jumps have small amplitude.

In steels, depending on the phase composition, strengthening effects can also be observed during the passage of current pulses. A similar strengthening effect during electropulsing (without deformation) was observed in medium carbon steel and ferritic-pearlitic steel [19]. The authors explained the strengthening in ferritic-pearlitic steel by structural refinement under the influence of current and proposed the corresponding mechanisms — an increased rate of nucleation in mild steel and spheroidization of cementite in the pearlite component. In St3 steel, the competition of existing mechanisms, dynamic recrystallization (initial softening due to increased dislocation density in ferrite) and low-cycle fatigue, is not excluded too.

Strengthening in this case during electropulsing can be associated with the dissolution of second-phase particles enriched in chromium or nickel and nanotwins in austenite [20]. The role of stacking fault energy in duplex (F + A) stainless steels remains unclear [21]. In our studies of austenitic-martensitic TRIP steel, duplex (F + M) steel, and steel 45, such an effect was not observed. On the contrary, in heat-hardened aluminum (AMg6) and copper (BrAZh9-4) alloys, the effects of strengthening were observed by us at a high duty cycle of the pulsed current.

5. Conclusions

All the above examples in alloys of completely different nature indicate the possibility of fixing not only the effects of softening, but noticeable effects of strengthening under the action of a pulsed current. A necessary condition for observing strengthening is a high duty cycle of the current, which makes it possible to suppress the influence of the thermal effect and reveal structural causes. These include dynamic deformation aging and recrystallization, martensitic transformations (caused by temperature or deformation), replacement of the dislocation slip mechanism by climbing, structure refinement, lattice defects generated by thermomechanical cycling (twins, stacking faults) [21, 22]. The possible reasons for the observed strengthening listed here should be confirmed by carefully performed structure studies, both by post-deformation methods and *in situ* observations.

Acknowledgments. This work was partially supported by the Ministry of Science and Higher Education of the Russian Federation in the frame work of agreement No. 075-15-2021-709 (unique project identifier RF-2296.61321X0037).

References

1. O. A. Troitskii. JETP Letters. 1, 18 (1969).
2. V. E. Gromov, L. B. Zuev, E. V. Kozlov, V. Ya. Tsellermayer. Electrostimulated plasticity of metals and alloys. Moscow, Nedra (1996) 280 p. (in Russian)
3. H. Conrad. Mater. Sci. Eng. A. 287, 276 (2000). Crossref
4. T. A. Perkins, T. J. Kronenberger, J. T. Roth. J. of Manufact. Sci. Eng. 129, 84 (2007). Crossref
5. W. A. Salandro, C. Bunget, L. Mears. ASME 2010 Conference (2010) 34043.
6. X. U. Chun, L. I. Ya-Nan, X. H. Rao. Trans. Nonferrous Met. Soc. China. 24, 3777 (2014). Crossref
7. Y. Zhou, G. O. Chen, X. S. Fu, W. L. Zhou. Trans. Nonferrous Met. Soc. China. 24, 1012 (2014). Crossref
8. H. Xie, Q. Wang, F. Peng, K. Liu, X. Dong, J. Wang. Trans. Nonferrous Met. Soc. China. 25, 2686 (2015). Crossref

9. T. Lee, J. Magargee, M.K. Ng, J. Cao. Inter. Journal of Plasticity. 94, 44 (2017). Crossref
10. A. Subrahmanyam, C. Shivaprasad, G. Suman, D.V. Raju, K.V. Rahul, R.N. Verkata. J. Manuf. Process. 75, 268 (2022). Crossref
11. K. Okazaki, M. Kagawa, H. Conrad. Mater. Sci. Eng. 45, 109 (1980). Crossref
12. C. Rudolf, R. Goswami, W. Kang, J. Thomas. Acta Mater. 209, 116776 (2021). Crossref
13. A.V. Pokoev, J.V. Osinskaya. Manifestation of Magnetoplastic Effect in Some Metallic Alloys. Defect Diffusion Forum. 383, 180 (2018). Crossref
14. H. Xu, X. Liu, Di. Zhang, X. Zhang. J. Mater. Sci. Technol. 35, 1108 (2019). Crossref
15. A.A. Shibkov, M.A. Zheltov, A.E. Zolotov, A.A. Denisov, M.F. Gasanov, D.V. Michlik. A method for increasing the mechanical stability and strength of aluminum-magnesium alloy sheet blanks using the effect of electroplastic deformation. Patent RU №2 624 87707.07. (2017). (in Russian)
16. V. Stolyarov. Europ. Symp. Martens. Transform. ESOMAT 2009 (2009) 06033. Crossref
17. S. Zhao, R. Zhang, Y. Chong et al. Nat. mater. 20, 468 (2021). Crossref
18. M.A. Pakhomov, V.V. Stolyarov. Metal Sci. Heat Treatment. 63, 236 (2021). Crossref
19. P. Long. J Phys. Conf. Ser. 1187 (3), 032054 (2019). Crossref
20. D.D. Ben, H.J. Yang, Y.R. Ma, X.H. Shao, J.C. Pang, Z.F. Zhang. Mater. Sci. Eng. A. 725, 28 (2018). Crossref
21. C. Gennari, L. Pezzato, E. Simonetto, R. Gobbo, M. Forzan, I. Calliari. Materials. 12, 1911 (2019). Crossref
22. O. Tyc, L. Heller, P. Sittner. Shap. Mem. Superelasticity. 7 (1), 65 (2021). Crossref